

# Effects of NK-4 in a Transgenic Mouse Model of Alzheimer's Disease

Hitomi Ohta\*, Shigeyuki Arai, Kenji Akita, Tsunetaka Ohta, Shigeharu Fukuda

Research Center, Hayashibara Biochemical Laboratories, Inc., Okayama, Japan

## Abstract

Beta-amyloid (A $\beta$ ) peptides are considered to play a major role in the pathogenesis of Alzheimer's disease (AD) and molecules that can prevent pathways of A $\beta$  toxicity may be potential therapeutic agents for treatment of AD. We have previously reported that NK-4, a cyanine photosensitizing dye, displays neurotrophic and antioxidant activities. In this study, we report the effects of NK-4 on the toxicity of A $\beta$  and on cognitive function and A $\beta$  concentration in a transgenic mouse model of AD (Tg2576). *In vitro*, NK-4 effectively protected neuronal cells from toxicity induced by A $\beta$ . In addition, it displayed profound inhibitory activities on A $\beta$  fibril formation. *In vivo*, Tg2576 mice received an intraperitoneal injection at 100 or 500  $\mu$ g/kg of NK-4 once a day, five times a week for 9 months. Administration of NK-4 to the mice attenuated impairment of recognition memory, associative memory, and learning ability, as assessed by a novel object recognition test, a passive avoidance test, and a water maze test, respectively. NK-4 decreased the brain A $\beta$  concentration while increasing the plasma amyloid level in a dose-dependent manner. NK-4 also improved memory impairments of ICR mice induced by direct intracerebroventricular administration of A $\beta$ . These lines of evidence suggest that NK-4 may affect multiple pathways of amyloid pathogenesis and could be useful for treatment of AD.

**Citation:** Ohta H, Arai S, Akita K, Ohta T, Fukuda S (2012) Effects of NK-4 in a Transgenic Mouse Model of Alzheimer's Disease. PLoS ONE 7(1): e30007. doi:10.1371/journal.pone.0030007

**Editor:** Hyoung-gon Lee, Case Western Reserve University, United States of America

**Received:** May 6, 2011; **Accepted:** December 9, 2011; **Published:** January 4, 2012

**Copyright:** © 2012 Ohta et al. This is an open-access article distributed under the terms of the Creative Commons Attribution License, which permits unrestricted use, distribution, and reproduction in any medium, provided the original author and source are credited.

**Funding:** Funding for this study was provided by Hayashibara Biochemical Laboratories Inc. The authors are employees of Hayashibara Biochemical Laboratories Inc., and they participated in study design, data collection, decision to publish and preparation of the manuscript.

**Competing Interests:** The authors are employees of, and funded by Hayashibara Biochemical Laboratories Inc. The Hayashibara Biochemical Laboratories Inc. assignees of a patent submitted for applications related to this work (International Patent Application No. PCT/JP2010/050927). This does not alter the authors' adherence to all the PLoS ONE policies on sharing data and materials. At the present moment, there are no products in development or marketed products that are associated with this study.

\* E-mail: htmohta@hayashibara.co.jp

## Introduction

Alzheimer's disease (AD) is the most common cause of dementia in elderly people and affects more than 25 million individuals worldwide. The development of therapeutic strategies for AD is a major unmet medical need. Inhibition of acetylcholinesterase (AChE) is currently a primary therapeutic strategy for the mid to late phase of AD because restitution of a close to normal acetylcholine concentration in the synaptic cleft to enhance cholinergic neurotransmission could ameliorate symptoms of AD. However, the therapeutic effect of AChE inhibitors is only symptomatic and short-term, and therefore new treatments are needed as disease-modifying therapy for AD.

Elevation of the levels of  $\beta$ -amyloid (A $\beta$ ), a ~4 kDa secreted polypeptide, is thought to be involved in the pathogenesis of AD because mutations in the A $\beta$  precursor protein (A $\beta$ PP) or presenilin genes that lead to increased production of A $\beta$  are causative for familial AD [1–8]. Elevated levels of A $\beta$  are also well correlated with cognitive decline in the early phase of dementia [9]. This indicates that suppression of A $\beta$  in the brains of patients in the early phase of dementia is a primary therapeutic target. The majority of new treatments aim to inhibit A $\beta$  toxicity. These include A $\beta$  immunotherapies that enhance clearance of accumulating A $\beta$  in brain and secretase inhibitors that inhibit production of A $\beta$  from A $\beta$ PP. Inhibitors of A $\beta$  aggregation are also currently under development, because the secondary structure determines

several important properties of A $\beta$  that may be relevant to the pathogenesis of AD.

The Tg2576 mouse model of AD expresses a high level of the Swedish mutation of A $\beta$ PP under control of the hamster prion protein promoter, which leads to elevated A $\beta$  production and accumulation in brain [10,11]. The Tg2576 strain does not exhibit aggressive neuronal degeneration, but the mice display age-dependent cognitive dysfunction [10,12–14] and are therefore an excellent tool for evaluation of A $\beta$ -targeted pharmacological agents.

NK-4 is a divalent cationic pentamethine trinuclear cyanine dye that contains three quinolinium rings, short N-alkyl side chains (C2) and two iodine anions. NK-4 has a variety of biological activities, including antimicrobial [15], macrophage-activating [16], and anticancer properties, and is used as an immunomodulator in treatment with antiviral and anticancer agents [17]. NK-4 also has anti-inflammatory properties [18] and has been used to treat allergy [19].

Recently, we found that NK-4 was a potent neurotrophic agent for promotion of growth and differentiation of neuronal PC12 cells. The neuroprotective effects of NK-4 are mediated by activation of PI3K-Akt and inactivation of SAPK/JNK independently of the TrkA receptor at nanomolar concentrations [20]. NK-4 is also a potent scavenger of hydroxyl radicals (IC<sub>50</sub>: 7.6  $\mu$ M), peroxy radicals (IC<sub>50</sub>: 5.2  $\mu$ M), and superoxides (IC<sub>50</sub>: 89.3  $\mu$ M), and these activities are greater than those of ascorbate

[21]. *In vivo*, NK-4 has been shown to be effective for cerebral injury in a rat model of middle cerebral artery occlusion [21] and for motor discoordination and cerebellar atrophy in a genetic animal model of cerebellar ataxia, without causing significant adverse reactions [20].

In the present study, we investigated the effects of NK-4 on AD *in vitro* and *in vivo*. We show that NK-4 is effective against A $\beta$ <sub>25–35</sub>-induced cytotoxicity in PC12 cells, and that NK-4 directly inhibits fibril formation of three forms of A $\beta$  peptide (A $\beta$ <sub>25–35</sub>, A $\beta$ <sub>1–40</sub> and A $\beta$ <sub>1–42</sub>). In A $\beta$ PP Tg mice, NK-4 significantly improved cognitive dysfunction in association with a substantial decrease in the A $\beta$ -immunoreactive tangles and A $\beta$  concentrations in the brain. Moreover NK-4 reversed cognitive impairments induced by an intracerebroventricular injection of A $\beta$ <sub>25–35</sub> in mice.

## Methods

### Chemicals

NK-4 (4,4'-[3-{2-(1-ethyl-4(1H)-quinolydene)ethylidene}propenylene] bis(1-ethylquinolinium iodide)) was synthesized at Hayashibara Biochemical Laboratories, Inc. (Okayama, Japan). A stock solution of 5 mg/ml NK-4 was prepared in DMSO and stored at room temperature with protection from light. Just before use, the stock solution was diluted with medium to give a 25  $\mu$ g/ml solution. This working solution was used for experiments with further dilution. A $\beta$ <sub>25–35</sub>, A $\beta$ <sub>1–42</sub> and A $\beta$ <sub>1–40</sub> were obtained from Anaspec (San Jose, CA). All other chemicals were purchased from Sigma-Aldrich (St. Louis, MO), unless otherwise indicated.

### Cell Culture

The rat pheochromocytoma cell line PC12 (Human Science Research Resources Bank, Osaka, Japan) was cultured in Dulbecco's Modified Eagle Medium (D-MEM; Nissui, Tokyo, Japan) supplemented with heat-inactivated 10% (v/v) fetal bovine serum and 5% (v/v) horse serum. For cell growth and neurite-outgrowth assays, PC12 cells were harvested using 0.1% (w/v) trypsin containing 0.03% (w/v) EDTA and seeded at a density of 5,000 cells/100  $\mu$ l in 96-well plates pre-coated with collagen type IV. After a 24 hr pre-culture, PC12 cells were exposed to A $\beta$ <sub>25–35</sub> (50  $\mu$ M) in the presence or absence of NK-4 for 72 hr. A $\beta$ <sub>25–35</sub> peptide were dissolved in DMSO (2 mM) and kept at  $-80^{\circ}$ C. Just before use, the solution was diluted in distilled water (200  $\mu$ M) and incubated at  $37^{\circ}$ C for 16 hr. This procedure, called "aging", promotes formation of stable oligomeric aggregates and enhances the cytotoxicity of the preparation. Cell survival was determined using alamarBlue dye (Trek Diagnostic Systems, Cleveland, OH) [22].

### Thioflavin T (ThT) Fibril Formation Assay

The A $\beta$  fibril formation assay was performed as described previously [23]. Stock solutions of A $\beta$ <sub>1–40</sub>, A $\beta$ <sub>1–42</sub> and A $\beta$ <sub>25–35</sub> were prepared in DMSO (1 mg/ml) and stored at  $-80^{\circ}$ C. Just before the experiment, the stock solution was diluted with 10 mM phosphate buffer containing 100 mM KCl (pH 7.4). The diluted A $\beta$  solutions were incubated at  $37^{\circ}$ C in the presence or absence of indicated concentrations of NK-4 for 72 hr. Fifty  $\mu$ l of the incubated samples containing 100  $\mu$ M A $\beta$  peptides were added to 450  $\mu$ l of 10  $\mu$ M ThT in 10 mM phosphate and 100 mM KCl (pH 7.4). Fluorescence intensity was measured with excitation at 435 nm and emission at 485 nm using a Hitachi 650-60 fluorescence spectrophotometer. The results are expressed as the mean  $\pm$  SD of three samples.

### Electron Microscopy

Amyloid fibril formation was verified by electron microscopy (EM) images of negatively stained samples. A 20- $\mu$ l sample of A $\beta$ <sub>1–40</sub> or A $\beta$ <sub>1–42</sub> solution incubated with or without NK-4 was placed on a polyvinyl butyral-coated copper mesh grid (Oukenshoji, Tokyo, Japan). The sample was allowed to stand for 30–60 s and excess solution was washed away. Subsequently, samples were negatively stained with 2% (w/v) uranyl acetate (Kowayakuhi, Saitama, Japan) and allowed to dry. After staining, the samples were viewed with a JEM-100CX/II electron microscope (Joel Ltd., Tokyo, Japan) at 80 kV.

### Animals

All animal protocols were approved by the Institutional Animal Care and Use Committee of Hayashibara Biochemical Laboratories (permit number F-1002) and were conducted in accordance with the guidelines for the Care and Use of Laboratory Animals at Hayashibara Biochemical Laboratories. Female A $\beta$ PP transgenic mice (Tg2576, 129S6/SvEvTac background) expressing a double mutation of human A $\beta$ PP [24], and age- and sex- matched non-transgenic mice were obtained from Taconic (Germantown, NY). The mice were housed individually with supplied nesting materials, and food and water were provided ad libitum. NK-4 solution was injected intraperitoneally at a dose of 100 or 500  $\mu$ g/kg once a day, five times a week for 9 months, beginning at 3 months of age. Control mice received 200  $\mu$ l of saline. During the behavioral test periods, NK-4 or saline was administered 2–3 hr before the start of each test. Male ICR mice (5 weeks of age, weighing 25–30 g) were purchased from Charles River Japan (Kanagawa, Japan).

### A $\beta$ <sub>25–35</sub>-Induced Cognitive Impairments in ICR Mice

Cognitive impairment was induced by a direct intracerebroventricular (icv) administration of aggregated A $\beta$ <sub>25–35</sub> peptide in mice according to the method described by Maurice et al. [25]. A $\beta$ <sub>25–35</sub> was dissolved in saline at the concentration of 1.0 mM and incubated at  $37^{\circ}$ C for 4 days, called "aging" process. On day0, aged A $\beta$ <sub>25–35</sub> solution (9 nmole/6  $\mu$ l/mouse) was injected by a micro-stainless needle (inner diameter: 0.13 mm) into the left lateral ventricle of ICR mice using following coordinates from Bregma: 0.5 mm posterior, 1.0 mm lateral, and 2.0 mm ventral. Sham operated mice received 6  $\mu$ l of saline instead of A $\beta$ <sub>25–35</sub> solution. From the next day of A $\beta$ -icv injection (day1), NK-4 solution was injected intraperitoneally at a dose of 50 or 500  $\mu$ g/kg/day for twelve consecutive days. Control mice received 200  $\mu$ l of saline. Mice were tested for object recognition and passive avoidance according to the methods described below during the day6–8 and day9–12, respectively.

### Novel Object Recognition Test

The task was carried out according to a previous report [26] with minor modification. The apparatus used in this study was an opaque plastic box (40 $\times$ 50 $\times$ 30 cm) with a clear acrylic cover plate on the top, the floor of which was covered with wood tips. The novel object recognition task comprised the following three sessions. First, in a habituation session, mice were individually placed in the box for 10 min of exploration in the absence of objects. Second, a training session was performed 24 hr after the habituation session. Two objects (A and B) were placed in the back corner of the box, 10 cm from the sidewall. Mice were individually placed in the middle front of the box and the time spent in exploring the two objects was recorded. Exploration behavior of the mice was defined as directing the nose toward the object at a

distance of less than 2 cm. Third, a retention session was performed 24 hr after the training session. One of the familiar objects (B) used in the training session was replaced by a novel object C, and objects A and C were placed as in the previous session. Mice were then individually placed in the box and allowed to explore freely for 10 min, with recording of the time spent in exploring each of the two objects. The exploratory preference was expressed as a ratio of the time spent exploring the novel object (TC) over that spent on the two objects (TA+TC): exploratory preference (%) =  $TC/(TA+TC) \times 100$ .

### Water Maze Test

A circular pool (diameter = 130 cm, Nishinohkoku, Okayama, Japan) was filled with water to a height of 15 cm. White ink was used to render the water opaque. The water temperature was maintained at  $23 \pm 1^\circ\text{C}$  throughout the trials. To enhance the positional recognition of mice, four different geometric patterns were placed at inner rim of each quadrant of the pool as well as each wall of the room. On the first day (day0), the platform (diameter = 9 cm) was placed at the midpoint of the pool, 0.5 cm above the water surface. Each mouse was placed on the platform and allowed to move away from the platform and swim in the pool for 15 sec, then gently guided to the original platform. The next day (day1), the platform was placed at the midpoint of one quadrant, submerged 0.5 cm below the water surface. The position of the platform was unchanged throughout the test trials. Two trials each day with an inter-trial interval of 1 min were conducted for 4 consecutive days (day1 to day4). In each trial, the mice were placed in the pool at one starting position, with their back turned to the midpoint of the pool. They were allowed to swim freely or until they found the hidden platform and came up for air while on the platform. The time required to escape onto the hidden platform was recorded as escape latency. If a mouse did not reach the platform within 120 sec, it was gently guided to the platform, where it remained for 10 sec. Starting locations were changed every trial. The results of 2 trials were averaged and used in data analysis.

### Passive Avoidance Test

A passive avoidance test was conducted using the apparatus consisted of two separate chambers ( $30 \times 30 \times 20$  cm height). One of the chambers was illuminated and the other was dark. Each chamber was separated by a small guillotine door ( $3.5 \times 5$  cm) and grids were attached on the floor in the dark chamber. This test comprised the following 3 sessions. First, in a pre-training session (day1 and day2), mice were individually placed in the illuminated chamber for 1 min and then in the dark chamber for 2 min. Second, in the test session (day3), mice were individually placed in the illuminated chamber. Immediately after the mice entered the dark chamber, the door was locked and an electrical stimulation of 0.36 mA was applied for 2 sec. The time spent in the illuminated chamber was measured. Third, in the retention session (day4), which was performed 24 hr later, mice were placed back in the illuminated chamber and the time spent in this chamber before entering the dark chamber was measured. The latency in the retention session was expressed graphically and used in data analysis.

### Measurement of A $\beta$ Species from Plasma and Brain Homogenates by ELISA

After mice were deeply anesthetized with pentobarbital (50 mg/kg), blood samples were withdrawn from the postcaval vein using heparinized syringe and the plasma was prepared and used fresh

or was stored at  $-80^\circ\text{C}$  until use. Cerebrospinal fluid (CSF) was collected from the dura mater over the cistern magna and brains were isolated. Hemi-brains were weighed and homogenized with a teflon-glass homogenizer in 20 mM Tris-buffered saline (TBS; 137 mM NaCl, protease inhibitor cocktail, pH7.6), and centrifuged at  $100,000 \times g$  for 1 hr at  $4^\circ\text{C}$ . Pellets were resuspended in TBS containing 2% SDS. After centrifugation at  $100,000 \times g$  for 1 hr at  $4^\circ\text{C}$ , the supernatant was obtained as the soluble fraction of A $\beta$ , and the pellet was extracted with 70% (w/v) formic acid, followed by centrifugation at  $100,000 \times g$  for 1 hr at  $4^\circ\text{C}$ . The supernatant was neutralized by 20-fold dilution with 1 M Tris base [27] and used as the insoluble A $\beta$  fraction. Samples were diluted with the diluents provided in the human (h)A $\beta_{1-40}$  and hA $\beta_{1-42}$  ELISA kits (Wako, Osaka, Japan). hA $\beta_{1-40}$  and hA $\beta_{1-42}$  in individual samples were quantified in accordance with the manufacturer's instructions and are expressed as picomoles/mL of plasma or picomoles/mg wet weight of brain (mean  $\pm$  SEM).

### Histology

Hemi-brains were fixed with 10% buffered formalin for 24 hr and embedded in paraffin blocks, and then coronal sections of cerebral cortex with 5  $\mu\text{m}$  thickness were stained with Congo-Red for counting amyloid plaques. For A $\beta$  immunohistochemistry, paraffin sections were dewaxed, rehydrated, and then blocked with PBS containing 0.2% Triton X-100 and 5% BSA. Sections were then incubated with rabbit anti-A $\beta$ -peptide polyclonal antibody (#71-5800, 1:50) (Invitrogen, Camarillo, CA) at  $4^\circ\text{C}$  overnight. After several washes in PBS, sections were incubated with HRPO-conjugated secondary antibody (DAKO, anti-rabbit Igs, 1:2000) and then A $\beta$ -immunoreactive tangles were visualized by diaminobenzidine.

### Statistical Analysis

All values are expressed as means  $\pm$  SD or SEM. A Student t test was used for comparison between 2 groups. One-way ANOVA with a Tukey-Kramer test was used to determine the significance of differences in multiple comparisons. In water maze, repeated measures two-way ANOVA followed by a post hoc Sheffe's F test was applied. Pearson correlation analysis was used to examine the correlation between A $\beta$  levels in plasma and brain in each mouse. Differences with a probability value of  $P < 0.05$  were considered to be significant.

## Results

### Effects of NK-4 against A $\beta$ -Induced Neurotoxicity in PC12 Cells

We first determined whether NK-4 was effective against A $\beta$ -induced neurotoxicity *in vitro* using PC12 cells. These cells (either undifferentiated or differentiated with nerve growth factor) are reported to be the most sensitive to A $\beta$  protein or the A $\beta_{25-35}$  fragment [28]. The cytotoxicity of A $\beta_{25-35}$  peptide is stronger than that of A $\beta_{1-40}$  in both PC12 cells and hippocampal neurons, which defined residues 25–35 as the active region of the A $\beta$  protein [28]. The cytotoxicity of A $\beta_{25-35}$  developed rapidly and was detected within 2 hr after application, and then reached a plateau after 72 hr of incubation (data not shown). The viability of PC12 cells treated with 50  $\mu\text{M}$  A $\beta_{25-35}$  for 72 hr was about 45% compared with controls without A $\beta_{25-35}$  (Fig. 1). NK-4 dose-dependently attenuated the effect of A $\beta_{25-35}$  and the results were significant at doses over 10 nM. NK-4 substantially reversed the cellular damage at 250 nM.

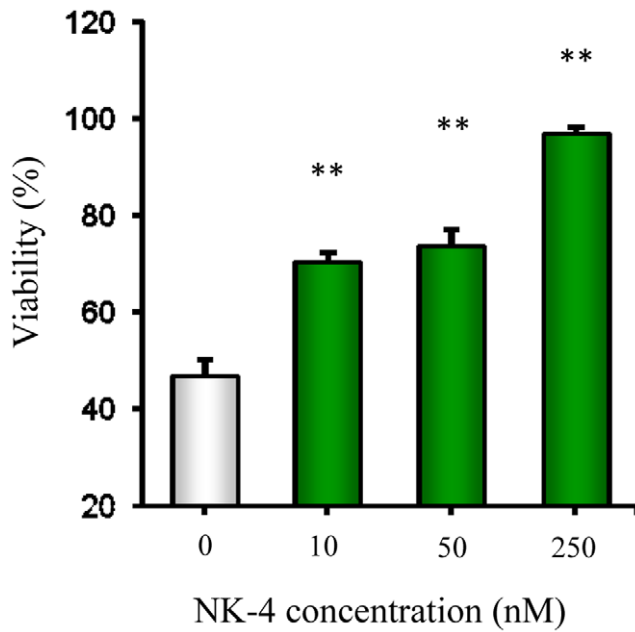


**Figure 1. Cytoprotective effects of NK-4 on  $A\beta_{25-35}$ -induced cytotoxicity in PC12 cells.** PC12 cells were treated with  $50 \mu\text{M}$   $A\beta_{25-35}$  for 72 hr in the absence (open bar) or presence of the indicated concentrations of NK-4 (closed bars). Control cells were incubated under the same conditions, but without  $A\beta_{25-35}$ . Cell viability was assessed by alamarBlue assay. Results are shown as means  $\pm$  SD (n=3). \*\*P<0.01 vs. no NK-4.  
doi:10.1371/journal.pone.0030007.g001

#### Effect of NK-4 on $A\beta$ Protein Fibrillization

To examine the potential mechanisms of NK-4-mediated protection of neuronal cells from amyloid toxicity, we evaluated the effect of NK-4 on aggregation or fibrillization of three forms of  $A\beta$  peptide. Solution of  $A\beta_{1-40}$  or  $A\beta_{1-42}$  ( $100 \mu\text{M}$  each) was incubated at  $37^\circ\text{C}$  for 3 days in the absence or presence of NK-4 at the indicated concentrations (Fig. 2). After the incubation, visible sedimentary aggregates were observed in the  $A\beta$  controls, while the addition of NK-4 had reduced visible aggregates. To examine the effect of NK-4 further, EM was used to monitor  $A\beta$  fibril formation. In EM,  $A\beta_{1-40}$  alone formed long and unbranched fibrils (Fig. 2a). In contrast,  $A\beta_{1-40}$  incubated with NK-4 ( $10 \mu\text{M}$ ) had shorter and fewer filaments with soluble assemblies (Fig. 2b). Similarly,  $A\beta_{1-42}$  formed dense fibrils (Fig. 2c) and they were remarkably weakened by the co-incubation with NK-4 (Fig. 2d). ThT fluorescence is enhanced upon binding to  $A\beta$  fibrils, proportionally to the amount of fibrils in solution [23]. So, we used ThT to evaluate the effect of NK-4 on the  $A\beta$  fibril formation quantitatively. All three forms of  $A\beta$  solutions showed enhanced emission at  $482 \text{ nm}$ , which is characteristic for ThT bound to amyloid fibrils. NK-4 inhibited all these ThT fluorescence dose-dependently (Fig. 2e). The inhibitory effect of NK-4 was most prominent on  $A\beta_{1-40}$ , then followed by  $A\beta_{1-42}$  and  $A\beta_{25-35}$ . An equimolar concentration of NK-4 almost totally inhibited the ThT fluorescence in all three forms of  $A\beta$ . These results suggest that NK-4 is an effective inhibitor of  $A\beta$  fibril formation *in vitro*.

#### Effects of NK-4 on Recognition Memory in the Novel Object Recognition Test

Given the beneficial effects of NK-4 on multiple aspects of amyloid pathology *in vitro*, we next examined whether NK-4 had

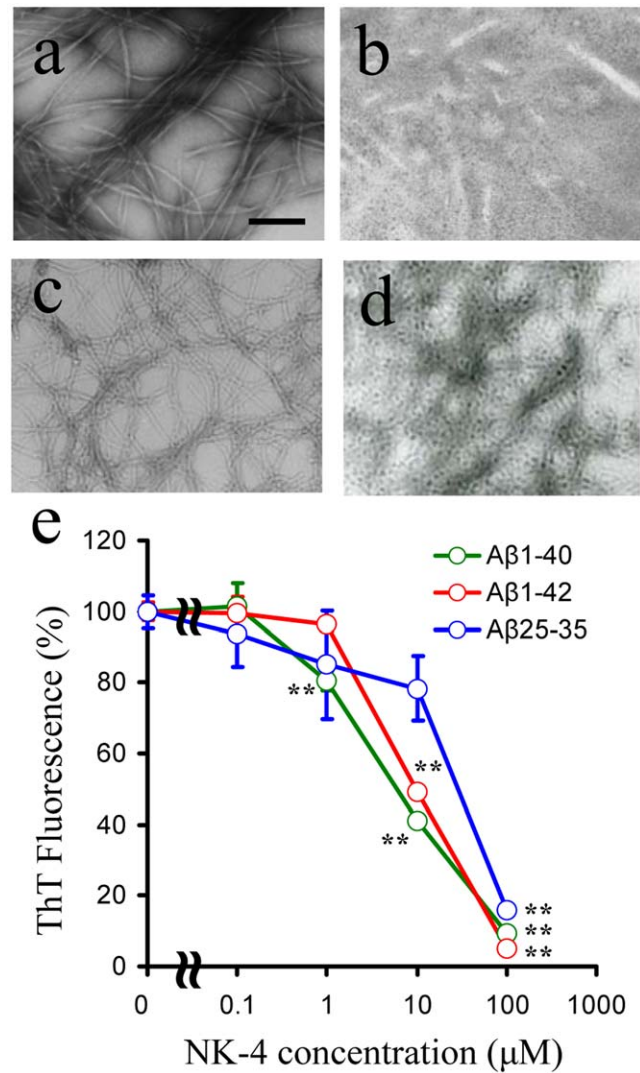


**Figure 2. Effects of NK-4 on  $A\beta$  fibril formation.**  $100 \mu\text{M}$  of  $A\beta_{1-40}$  (a, b) or  $A\beta_{1-42}$  (c, d) was incubated for 72 hr alone (a, c) or with NK-4 ( $10 \mu\text{M}$ ) (b, d). Bar represents  $200 \text{ nm}$ . The experiment was performed three times with similar results. (e) Thioflavin T assay of  $A\beta$  fibril formation. Three forms of  $A\beta$  peptide ( $A\beta_{1-40}$ ,  $A\beta_{1-42}$  and  $A\beta_{25-35}$ ) were incubated for 72 hr with the indicated concentration of NK-4. Values are means  $\pm$  SD (n=3). \*\*P<0.01 vs. control (without NK-4).  
doi:10.1371/journal.pone.0030007.g002

an effect on the cognitive deficit induced by  $A\beta$  in an  $A\beta\text{PP}$  transgenic mouse model of AD. Tg2576 mice expressing the Swedish mutation of  $A\beta\text{PP}$  were administered with  $100$  or  $500 \mu\text{g/kg}$  NK-4 once a day, 5 times a week for 9 months, beginning at 3 months of age. Wild type and Tg2576 mice were tested for object recognition memory 24 hr after training to test long-term memory at ages 3, 6 and 12 months. During the training session, there were no significant differences in exploratory preference between the two objects or in the total exploratory time among the groups (data not shown). At 3 months of age, we could not detect significant differences in recognition memory among all groups tested (data not shown). In the retention session, Tg2576 mice at ages 6 and 12 months showed significantly decreased object recognition memory compared with that in the wild type mice at the respective ages (Fig. 3). Tg2576 mice treated with a low dose of NK-4 ( $100 \mu\text{g/kg}$ ) tended to spend a longer

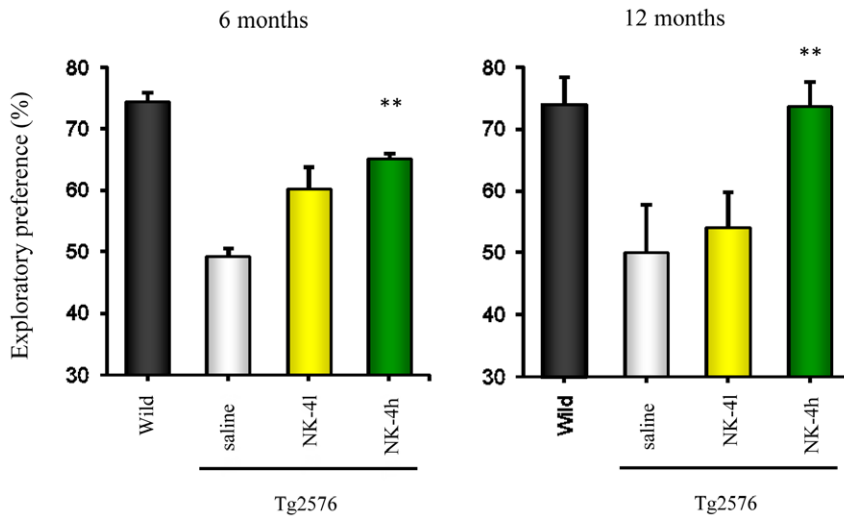


**Figure 3. Effects of NK-4 on cognitive function of Tg2576 mice in a novel object recognition test.** A low (100  $\mu\text{g}/\text{kg}$ ) or high (500  $\mu\text{g}/\text{kg}$ ) dose of NK-4 was administered intraperitoneally to female Tg2576 mice from 3 to 12 months of age. Mice were tested for object recognition at 6 and 12 months of age. Values are means  $\pm$  SEM ( $n = 10$ ). \*\* $P < 0.01$  vs. saline-treated Tg2576 group. Wild: non-transgenic female 129S6 mice. Tg2576 (saline): saline-treated Tg2576 mice. Tg2576 (NK-4l): low-dose NK-4-treated Tg2576 mice. Tg2576 (NK-4h): high-dose NK-4-treated Tg2576 mice. doi:10.1371/journal.pone.0030007.g003

time exploring the novel object than did the saline-treated controls at both 6 and 12 months of age (treated for 3 and 9 months), but the differences were not significant. In contrast, Tg2576 mice treated with a high dose of NK-4 (500  $\mu\text{g}/\text{kg}$ ) spent a significantly longer time exploring the novel object than did the saline-treated mice at both 6 and 12 months of age, and the exploratory preference was comparable to that of wild type controls at age 12 months (after 9 months treatment). This suggests that NK-4 administration for a longer period might be more effective for improvement of object recognition memory.

#### Effects of NK-4 on Learning Ability in the Water Maze Test

We also evaluated learning ability of mice in a water maze test at ages 6 and 12 months (Fig. 4). Group differences in the escape

latency of the training trial session were analyzed using two-way ANOVA with repeated measures. There were significant differences in escape latency between genotype (wild type controls vs. saline-treated Tg2576 mice) at 6 months of age [Genotype  $\times$  Time  $F(1,54) = 40.531$ ,  $P < 0.001$ ], and at 12 months of age [Genotype  $\times$  Time  $F(1,48) = 7.269$ ,  $P < 0.05$ ]. For saline-treated Tg2576 group, the latency to reach the platform did not shorten during the whole test period at 12 months of age. There was a significant Genotype  $\times$  Time interaction [ $F(3,48) = 5.0732$ ,  $P < 0.01$ ] at this stage, suggesting that the learning ability of saline-treated Tg2576 mice became impaired with age.

We found significant differences in escape latency between treatments (NK-4 vs. saline) at 6 months of age [Group  $\times$  Time  $F(2,81) = 10.404$ ,  $P < 0.001$ ], and at 12 months of age [Group  $\times$  Time  $F(2,75) = 5.671$ ,  $P < 0.01$ ]. The interaction of the grouping

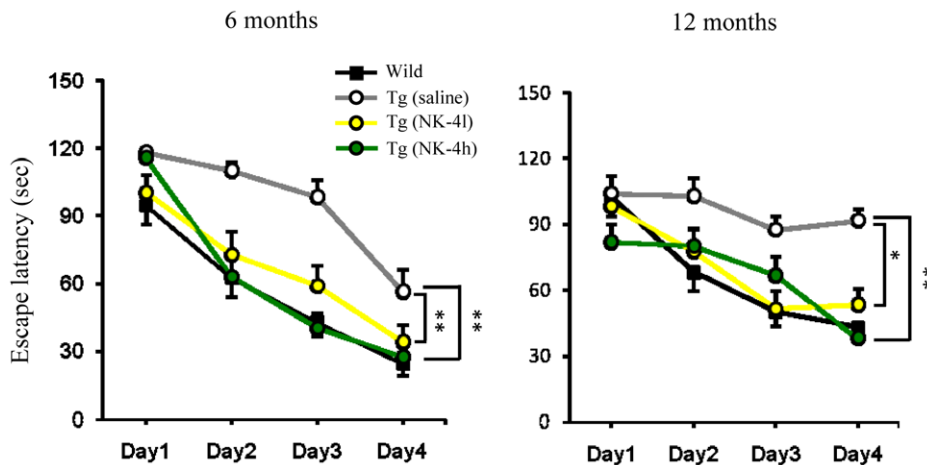


**Figure 4. Effect of NK-4 on learning ability of Tg2576 mice in a water maze test.** Mice were tested for learning ability at 6 and 12 months of age. The mean latency represents the time spent finding a hidden platform placed in a fixed location in the pool. Two trials per day were conducted for 4 consecutive days. Data are expressed as means  $\pm$  SEM of the averaged time on each day ( $n = 10$ ). \* $P < 0.05$ , \*\* $P < 0.01$  vs. saline-treated Tg2576 group. doi:10.1371/journal.pone.0030007.g004

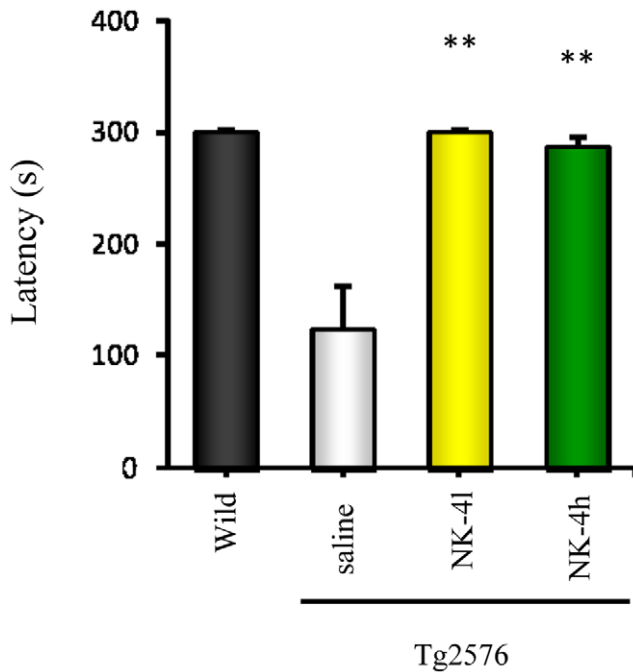


**Figure 5. Effect of NK-4 on cognitive function of Tg2576 mice in a passive avoidance test.** Mice were tested for learning at 9 months of age. The latency in the retention session performed 24 hr after the training session is shown. Values are means  $\pm$  SEM (n=10). \*\*P<0.01 vs. saline-treated Tg2576 group. doi:10.1371/journal.pone.0030007.g005

factor and the time factor also proved to be significant at 6 months of age [ $F(6,81) = 2.672$ ,  $P<0.05$ ]. Saline-treated Tg2576 group consistently exhibited a longer latency than NK-4-treated Tg2576 groups. Both low (100  $\mu\text{g}/\text{kg}$ ) and high (500  $\mu\text{g}/\text{kg}$ ) doses of NK-4 improved learning ability of Tg2576 mice with significant differences compared with saline-treated controls ( $P<0.01$  at 6 months of age,  $P<0.05$  at 12 months of age), but the effects of NK-4 on escape latency did not differ significantly between these two doses. The swimming ability did not differ significantly among Tg2576 groups (data not shown).

#### Effects of NK-4 on Passive Avoidance Memory

Recognition memory of NK-4-treated mice at ages 3 and 9 months was evaluated in a passive avoidance test. Similar to the novel object recognition test, no significant difference was detected in latencies for entering the dark chamber of a passive avoidance apparatus during the retention session among all groups tested at 3 months of age (data not shown). However at 9 months, there was a significant difference in latencies between wild type control and saline-treated Tg2576 mice ( $p<0.01$ ). Both low (100  $\mu\text{g}/\text{kg}$ ) and high (500  $\mu\text{g}/\text{kg}$ ) doses of NK-4 reversed the decrease in passive avoidance latency of Tg2576 mice, and the differences were significant compared with saline-treated controls (both  $p<0.01$ , Fig. 5). There was no difference in latencies for entering the dark chamber between wild type and Tg2576 mice, or among the treatment groups after placement in the light chamber for the first time during the training session (in the absence of shock). All animals took an average of 70 s to move to explore the dark chamber, indicating no baseline differences in anxiety in the treatment groups in this behavioral test. We also found no difference in shock sensitivity among wild type and saline- and NK-4-treated Tg2576 mice.

#### Effect of NK-4 on A $\beta$ Levels in Tg 2576 Mice

We next evaluated whether NK-4 displayed any significant effect on A $\beta$  levels in plasma, CSF and brains from Tg2576 mice. Since NK-4 might directly interact with A $\beta$  peptides, we examined whether it interferes the A $\beta$  ELISA. Although the presence of NK-4 slightly enhanced optical density values in A $\beta$  ELISA systems, the range of increase was less than 5% when the NK-4:A $\beta$  molar ratio was 0.1~100 (Fig. 6a, b). This indicated that NK-4 hardly affects both A $\beta_{1-40}$  and A $\beta_{1-42}$  ELISA systems.

Dose-dependent increases in A $\beta_{x-40}$  and A $\beta_{x-42}$  were observed in plasma from NK-4 treated mice (Fig. 6c, d). In contrast, CSF A $\beta_{x-40}$  and A $\beta_{x-42}$  levels were not significantly changed by NK-4 treatment, although the CSF concentrations of A $\beta_{x-40}$  and A $\beta_{x-42}$  in NK-4 treated mice tended to be lower than those in saline-treated controls (data not shown). Brain levels of A $\beta$  were estimated separately in soluble and insoluble fractions. Both soluble and insoluble A $\beta_{x-40}$  levels were significantly decreased by NK-4 treatment (Fig. 7a, c). Similarly, levels of A $\beta_{x-42}$  were lower in NK-4 treated mice, with a significant decrease in insoluble A $\beta_{x-42}$  (Fig. 7b, d). The levels of A $\beta_{x-40}$  and A $\beta_{x-42}$  in brain were inversely correlated with those in plasma ( $r = -0.69$ ,  $P<0.01$  (n = 27), and  $r = -0.42$ ,  $P<0.05$  (n = 27), respectively) (Fig. 7e, f).

We next surveyed brain A $\beta$  deposition of Tg2576 mice by Congo Red (CR) staining and A $\beta$  immunohistochemistry (Fig. 8). Wild type mice did not show any sign of amyloid deposition in their brain at 12 month of age (Fig. 8a). Tg2576 mice at the same age developed distinguishable, but very few amount of plaques in their cortex region. The number of CR-positive plaques in the cerebral cortex region was not significantly changed among saline-treated group and NK-4-treated groups (Fig. 8a). On the contrary, A $\beta$ -immunoreactive small tangles were abundantly seen in the cortex of saline-treated Tg2576 mice (Fig. 8b), and they were obviously reduced by the high dose NK-4 treatment both in size and in quantity (Fig. 8c).

#### Effects of NK-4 on A $\beta_{25-35}$ -Induced Cognitive Impairment in ICR Mice

To confirm whether the effect of NK-4 was directly attributable to mitigation of A $\beta$  pathology, we employed an A $\beta$ -induced amnesia model, in which ICR mice received intracerebroventricular (icv) administration of aged A $\beta_{25-35}$  peptide to provoke memory deficits [25]. Long-term recognition memory was evaluated by the novel object recognition test and the passive avoidance test starting at 6 days and 9 days after A $\beta_{25-35}$ -icv injection, respectively. In both behavioral assays, daily NK-4 treatment dose-dependently, and significantly improved the memory deficits induced by A $\beta$  (Fig. 9a, b). These results, in combination with the results from Tg2576 mice, strongly suggested that NK-4 treatment improved A $\beta$ -mediated memory impairments.

#### Discussion

NK-4 is a N-heterocyclic cationic dye derivative that contains three quinolinium rings and two iodine anions. Although NK-4 shows a variety of biochemical and biological activities [15–21], structure-activity relationships or molecular mechanisms of them remain largely unknown. Extended  $\pi$ -electron conjugated system of NK-4 would considerably contribute to antioxidative effects by trapping free radicals similar to another cyanine dye platinon [29]. The extended conjugated system also confers this molecule a planar structure by which NK-4 seems to bind at the interface of the  $\beta$ -sheet domains of the proteins and act as a “ $\beta$ -sheet breaker” [30]. On the other hand, it is reported that the side chain length affects

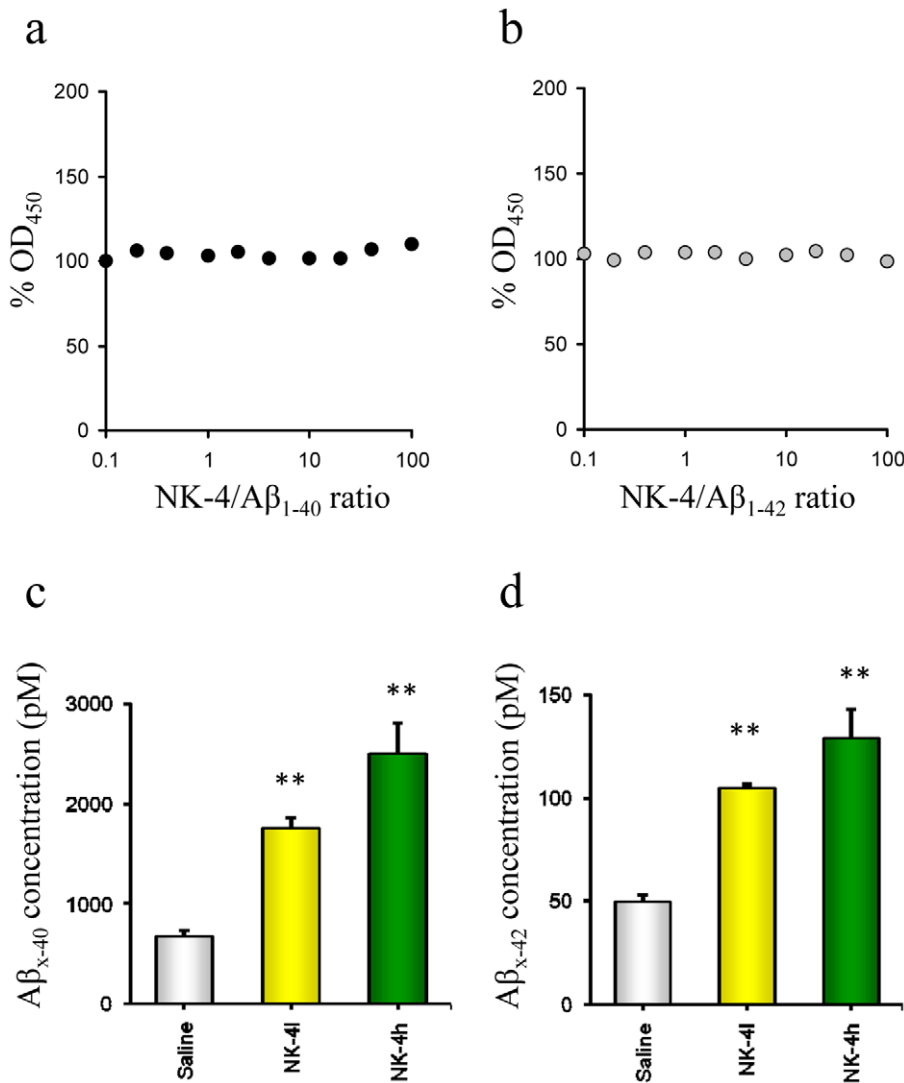


**Figure 6. Effect of NK-4 on the plasma Aβ concentrations in Tg2576 mice.** NK-4 did not interfere the optical density of both hAβ<sub>1-40</sub> (a) and hAβ<sub>1-42</sub> (b) ELISA systems, which using the antibody combinations of BAN50/BA27 and BAN50/BC05, respectively. Since these ELISA systems cannot distinguish N-terminal heterogeneity of Aβ peptides derived from biological samples, we represented hAβ species as hAβ<sub>x-40</sub> and hAβ<sub>x-42</sub>, respectively. Plasma from mice aged 12 months was used for measurements of hAβ<sub>x-40</sub> (c) and hAβ<sub>x-42</sub> (d). Values are the mean ± SEM for saline-treated Tg2576 mice (control group, n = 10), a low dose NK-4 (100 μg/kg)-treated group (n = 9), and a high dose NK-4 (500 μg/kg)-treated group (n = 8). \*\*P < 0.01 vs. saline-treated Tg2576 group. doi:10.1371/journal.pone.0030007.g006

water solubility or affinity to the lipid membrane in this kind of dye compounds [31]; therefore, the specific activity of NK-4 might change in accordance with the length of N-alkyl side chains.

Application of neurotrophic small molecules that modulate neuronal survival and synaptic function is a promising therapeutic approach for AD, while modulation of the amyloid pathology is a key strategy for slowing or halting the disease progression. In this study, we showed that NK-4 protected neuronal cells from Aβ<sub>25-35</sub>-induced toxicity (Fig. 1). Attenuation of Aβ cytotoxicity by NK-4 might be caused by direct action on Aβ to prevent its aggregation into more toxic forms, or via activation of intracellular survival signaling pathways and inactivation of death pathways in neuronal cells [20], or both. The effect of NK-4 on Aβ fibril formation was significant, but the IC<sub>50</sub> value for Aβ aggregation was approximately 10 μM for Aβ<sub>1-40</sub> and Aβ<sub>1-42</sub>, and 30 μM for Aβ<sub>25-35</sub> (Fig. 2e). In contrast, a much lower concentration (nM level) of NK-4 attenuated the neurotoxicity induced by 50 μM

Aβ<sub>25-35</sub> in PC12 cells (Fig. 1). These results suggest that NK-4 attenuates Aβ-induced toxicity via activation of intracellular survival signaling pathways including Akt activation [20], rather than direct inhibition of Aβ aggregation, since the concentration of NK-4 required inhibiting Aβ aggregation was substantially high. However, the effect of NK-4 on Aβ aggregation was greater than those of non steroidal anti-inflammatory drugs (NSAIDs) such as ibuprofen, naproxen, ketoprofen, and indomethacin [32,33], which require at least a threefold higher concentration to inhibit Aβ aggregation. Therefore, the anti-fibrillization effect of NK-4 might play some role in attenuating Aβ toxicity *in vivo*.

Chronic administration of NK-4 to Tg2576 mice significantly attenuated cognitive decline as assessed in a set of behavioral tests (Fig. 3,4,5), and also decreased the levels of Aβ in brain (Fig. 7) and augmented those in plasma (Fig. 6). These results imply that the NK-4-induced behavioral improvement was attributable to decreased Aβ in brain, and that Aβ may be cleared across the

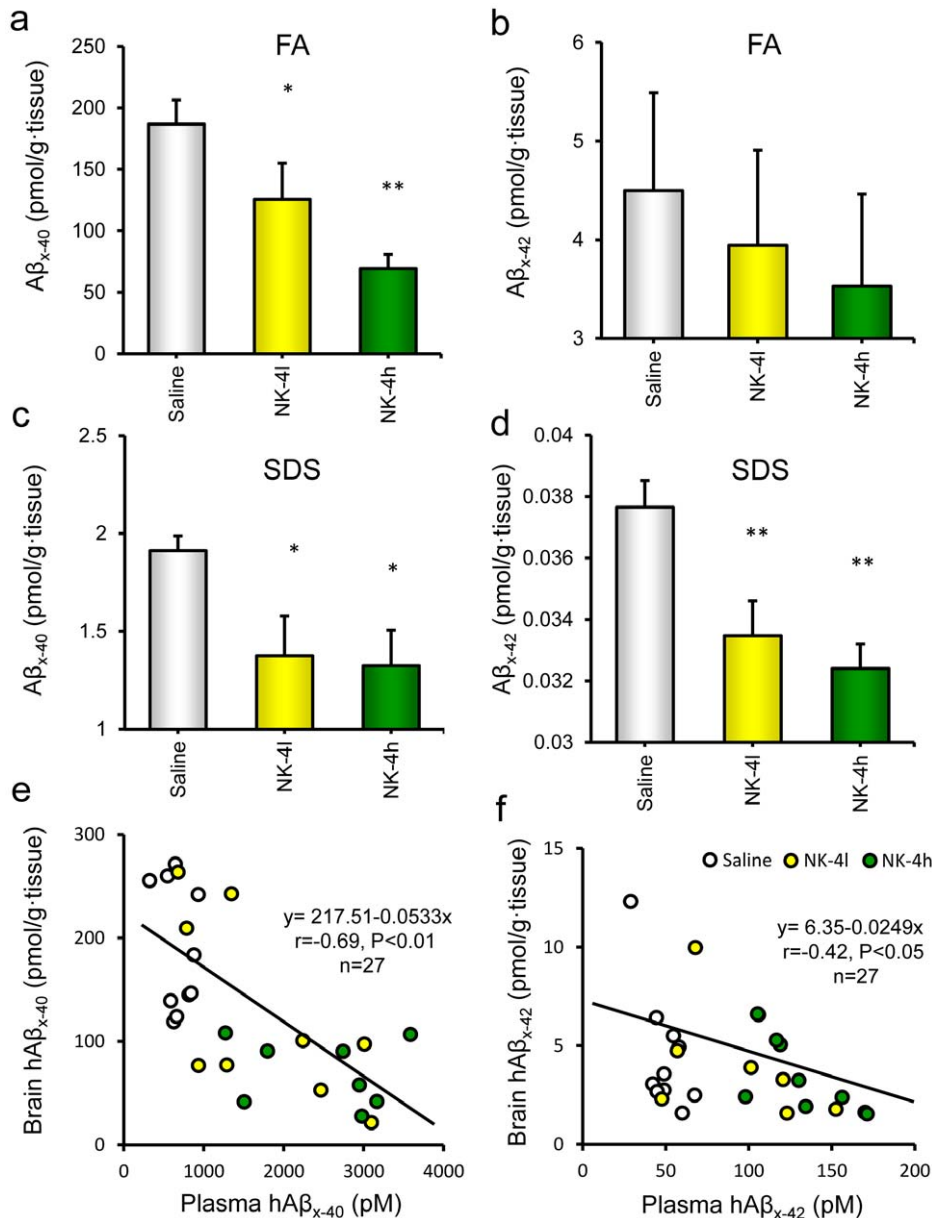


**Figure 7. Effect of NK-4 on brain soluble or insoluble  $A\beta_{x-40}$  and  $A\beta_{x-42}$  in Tg2576 mice.** Brains from mice aged 12 months were homogenized and separated into soluble (c, d) and insoluble (a, b) fractions of  $A\beta$ , and assayed for  $hA\beta_{x-40}$  (a, c) and  $hA\beta_{x-42}$  (b, d), respectively. FA: SDS insoluble and formic acid soluble fractions of  $A\beta$ . SDS: SDS soluble fractions of  $A\beta$ . Correlations are shown between the plasma and brain levels of  $hA\beta_{x-40}$  (e) and  $hA\beta_{x-42}$  (f) in Tg2576 mice. Data are the mean  $\pm$  SEM of  $hA\beta_{x-40}$  or  $hA\beta_{x-42}$  in each mouse in saline-treated Tg2576 controls ( $n = 10$ ), a low dose NK-4 (100  $\mu\text{g}/\text{kg}$ )-treated group ( $n = 9$ ), and a high dose NK-4 (500  $\mu\text{g}/\text{kg}$ )-treated group ( $n = 8$ ). \* $P < 0.05$ , \*\* $P < 0.01$  vs. saline-treated Tg2576 group.

doi:10.1371/journal.pone.0030007.g007

blood-brain barrier to the blood. A similar large increase in plasma  $A\beta$  was found after peripheral administration of an anti- $A\beta$  antibody in an AD mouse model [34]. Although there is still no consensus as to the mechanism by which anti- $A\beta$  antibodies alter amyloid deposition, *in vivo* binding properties of the antibodies would affect plasma  $A\beta$  levels by altering the half-life of  $A\beta$  [34]. In a similar fashion, a direct NK-4 binding to  $A\beta$  in Tg2576 mice may be one possible explanation of augmented plasma  $A\beta$  levels by chronic peripheral administration of NK-4. On the other hand, plasma might serve as a sink that enhances clearance of  $A\beta$  from the brain based on a peripheral sink hypothesis [35,36], because  $A\beta$  clearance mainly occurred in plasma in Tg2576 mice [34]. It

might be also possible that direct NK-4 binding to  $A\beta$  creates a sink that enhances clearance of  $A\beta$  deposition from brain. In either case, further study is required to address these issues.

It seems unlikely that the impaired performance of Tg2576 mice in learning and memory tests is due to changes in motivation or sensorimotor function, since the motivation for each behavioral test is different and different skills are required for a good performance in each test. There were no differences in locomotor activity, total time spent exploring objects in the novel object test between wild type and Tg2576 mice. Recognition memory in the novel object test and associative learning in the passive avoidance test are dependent on the hippocampus and/or perirhinal cortex

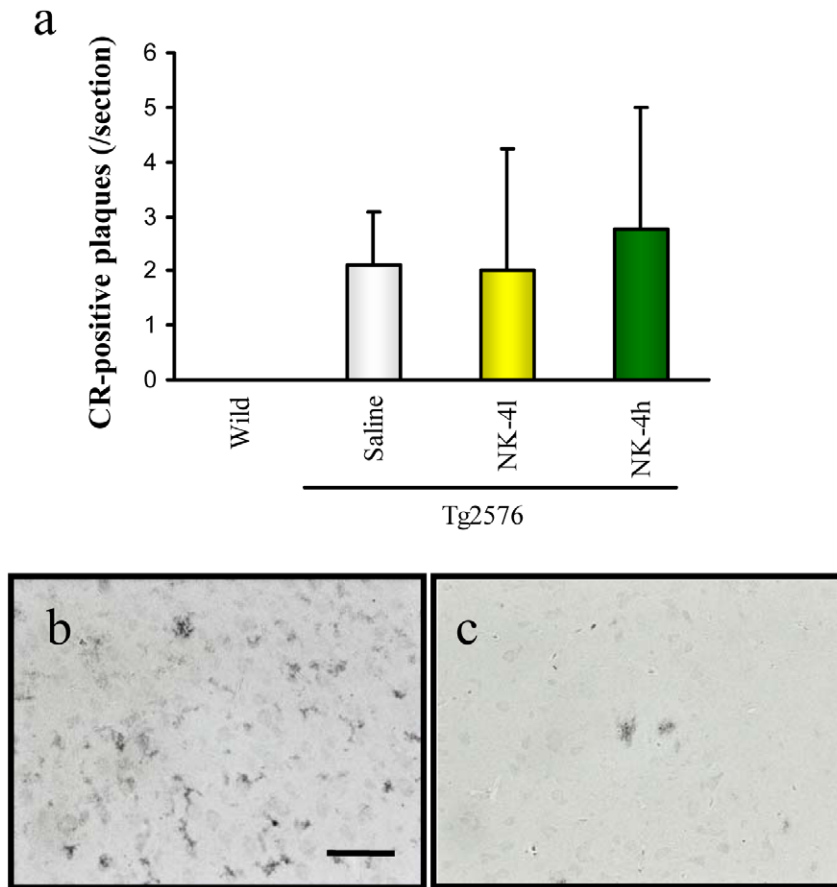


**Figure 8. A $\beta$  deposition in brains of Tg2576 mice at 12 months of age.** Coronal brain sections (cortex region) were stained by Congo Red (a) or anti-A $\beta$  polyclonal antibody (b, c). The number of CR-positive plaques on the section was counted in cortex region (a). Typical images of A $\beta$ -immunoreactive tangles of saline-treated Tg2576 mouse (b) and high-dose NK-4(500  $\mu$ g/kg)-treated Tg2576 mouse (c). Bar represents 50  $\mu$ m. doi:10.1371/journal.pone.0030007.g008

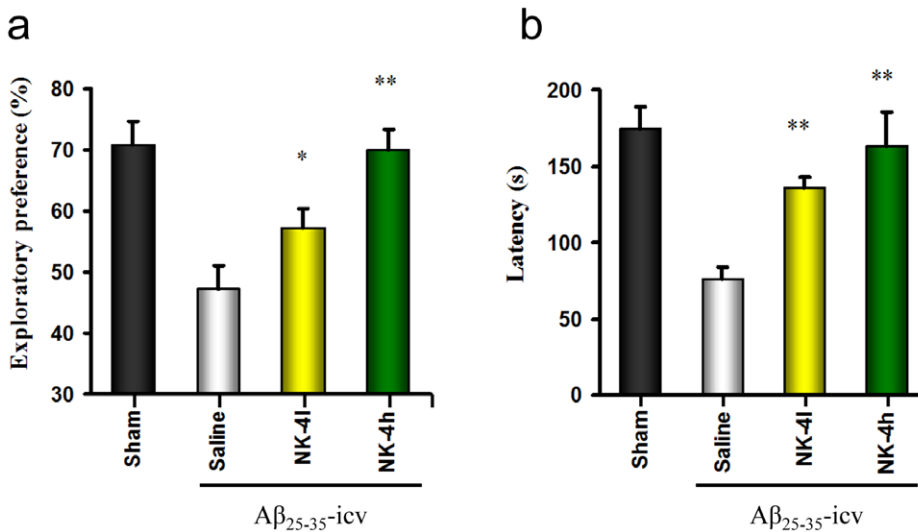


**Figure 9. Effects of NK-4 on A $\beta_{25-35}$ -induced cognitive impairments in ICR Mice.** Cognitive impairment was induced in ICR mice by icv injection of A $\beta_{25-35}$  solution as described in Material and Method. A low (50  $\mu$ g/kg) or high (500  $\mu$ g/kg) dose of NK-4 was administered intraperitoneally to mice twelve consecutive days starting from the next day of A $\beta$  injection (day1). Mice were tested for object recognition (a), followed by passive avoidance (b). Values are means  $\pm$  SEM (n = 10). Sham: sham-operated group, saline: saline-treated A $\beta_{25-35}$ -icv group, NK-4l: low-dose NK-4-treated A $\beta_{25-35}$ -icv group, NK-4h; high-dose NK-4-treated A $\beta_{25-35}$ -icv group. \*P<0.05, \*\*P<0.01 vs. saline-treated group. doi:10.1371/journal.pone.0030007.g009

[37–39]. In this context, progressive impairment of the hippocampus and/or perirhinal cortex-dependent memory started as early as 6 months of age and continued to 12 months of age in Tg2576 mice in our experiment. Contrary to this, histological investigation of A $\beta$  deposits in Tg2576 mice showed no substantial differences in quantity of CR-positive plaques among the saline-treated group and NK-4-treated groups at 12 month of age (Fig. 8a). On the other hand, A $\beta$ -immunoreactive tangles were abundant in the cortex of saline-treated Tg2576 mice and they were clearly decreased by high dose NK-4 treatment in good agreement with the results of A $\beta$  ELISAs (Fig. 7, Fig. 8b, c), and it might also reflect the cognitive function (Fig. 3, 4). The difference in plaque stainability between CR and anti-A $\beta$  would be due to the sensitivity to immature tangles, and therefore, CR staining might not reflect the total amount of A $\beta$  deposition in brain.

The Tg2576 mouse is the most thoroughly characterized AD mouse model and is considered to reflect the human amyloid pathology most closely among mouse models [11]. Although many studies using mice on a B6/SJL background (hereafter; Tg2576/B6), we used here the newly developed 129S6/SvEvTac strain (hereafter; Tg2576/129) established by Taconic, because this strain does not carry a retinal degeneration mutation [24]. The 129 strains are reported not appropriate for water maze tasks according to previous studies [40–43], however, the wild type mice of 129S6/SvEvTac strain performed well in the acquisition learning of water maze test [44]. Regarding the timing of cognitive decline, our results showed that the Tg2576/129 did not exhibit cognitive decline at the age of 3 months (data not shown), but became apparent at 6 months, which continued to 12 months (Fig. 3,4,5). Reportedly, Tg2576/B6 showed no detectable cognitive impairment at 3–4 months, but became obvious at 5–6 months of age [14,45–47]. Thus, genetic backgrounds appear not to be affected in the timing of cognitive decline.

The water maze protocol we employed in this study is a variant of Morris water maze navigation task. Although the original protocol was designed for evaluating hippocampus-dependent spatial reference learning and memory [48], our modified protocol is not considered as the one for spatial cognition since we used extra intra-maze landmarks and did not run a probe trial. We placed proximal landmarks on the inner rim of the pool in addition to each wall of the room (distal landmarks) aiming to enhance positional recognition of mice, however, it is suggested that the processing of information related to distal landmarks (room cues) or proximal landmarks (intra-maze cues) are mediated by different neural systems [49,50]. The hippocampus circuitry contributes to a spatial strategy, which involves flexible use of spatial/distal cues, whereas a cue strategic processing of proximal landmarks is dependent upon striatal circuitry [50]. Thus, what we evaluated using the extra proximal landmark condition would not be spatial reference learning, but non-spatial or mixture of both. On another note, the lack of probe trial made it difficult to confirm the memory retention. As a result of these modified experimental design, we could not determine whether the learning strategy of the mice was spatial or not. One thing for certain is, however, that NK-4 modulated the learning ability of Tg2576/129 mice in the water maze task (Fig. 4). The learning ability of Tg2576/129 mice was impaired with age, and a long-term NK-4 treatment significantly improved it. Results of two other behavioral tests (Fig. 3, Fig. 5) support this notion.

In relation to the learning ability of the mice on 129 background, it has been known that all 129 mouse substrains have disrupted-in-schizophrenia 1 (*DISC1*) deletion mutation [51]. Because *DISC1* is reported to play a critical role in development and migration of hippocampal neurons [52], cognitive deficits observed in 129 strains

may linked to lack of *DISC1* protein. In this regard, preferable effect of NK-4 on cognitive improvements of Tg2576/129 mice may be attributable to restoring the dysfunctional *DISC1*-mediated pathway. To address this question, we examined the effect of NK-4 on A $\beta$ -dependent amnesic mice model [25]. As a result, NK-4 treatment dose-dependently and significantly attenuated memory dysfunction induced by direct injection of A $\beta$ <sub>25–35</sub> peptide into the lateral ventricle of ICR mice (Fig. 9). Therefore, the modification of *DISC1*-mediated pathway by NK-4 seems not mainly involved in this case. Since NK-4 activated PI3K-Akt pathway independently of the TrkA receptor *in vitro* [20], activated Akt (p-Akt) may be an important mediator of the beneficial effects on learning and memory. The p-Akt is required for PI3K-mediated synaptic plasticity and memory consolidation by promoting neuronal cell survival and protein synthesis via phosphorylation of CREB, a downstream regulator involved in hippocampus-dependent long-term and spatial memory formation [53]. Therefore, induction of Akt phosphorylation might play critical roles in NK-4-mediated memory improvement in Tg2576/129 mice.

Oxidative mechanisms are also thought to be involved in the cell loss and other neuropathology associated with AD [54,55]. In AD pathogenesis, reactive oxygen species (ROS) impair mitochondrial redox activity and increases further ROS generation [29,56,57]. A $\beta$  induces production of ROS and leads to apoptotic neuronal cell death that can be inhibited by antioxidants [57–59]. Pathologic and biochemical studies suggest that ROS induced by fibrillar A $\beta$  have neurotoxic effects [60,61]. As mentioned before, NK-4 is a potent scavenger of ROS [21] and an inhibitor of A $\beta$  aggregation (Fig. 2). Those activities might contribute to attenuation of A $\beta$  toxicity in AD.

As to the safety profile, NK-4 was well tolerated in a mouse acute oral toxicity study at up to 2 g/kg [21], based on mortality, clinical observations, body weight, hematology, blood chemistry, organ weights, and histological examinations of a full tissue list. Additionally, NK-4 was not mutagenic in the standard Ames test due to bacterial-specific metabolism (data not shown). Furthermore, there were no specific adverse events in mice those received intraperitoneal injections of NK-4 at the dose of up to 500  $\mu$ g/kg/day, 5 days a week, for 9 months (this study). These observations suggest that NK-4 is a safe compound that will not cause serious adverse reactions. Following an intraperitoneal administration at 500  $\mu$ g/kg, NK-4 penetrated the brain and nM levels were detected using high-performance liquid chromatography [20]. Thus, the nM range used in the *in vitro* investigations in this study corresponds to the calculated brain concentration in Tg2576/129 mice receiving NK-4.

In summary, the results of this study show that chronic treatment with NK-4 from an early stage of cognitive dysfunction significantly ameliorated learning impairments in Tg2576/129 A $\beta$ PP mouse. The NK-4-induced behavioral improvement might be attributable to decreased A $\beta$  accumulation in brain, and the inhibitory effects on A $\beta$  aggregation, neurotrophin-like property, as well as radical-scavenging effect of NK-4. Its multiple functions might work in concert to attenuate AD pathology.

## Acknowledgments

We would like to thank Dr. Makoto Takeuchi (Cell Biology Institute, Hayashibara Biochemical Laboratories, Inc.) for supporting the EM study.

## Author Contributions

Conceived and designed the experiments: HO SA KA TO SF. Performed the experiments: HO SA KA. Analyzed the data: HO KA. Contributed reagents/materials/analysis tools: HO SA KA. Wrote the paper: HO KA TO.

## References

- Goate A, Chartier-Harlin M, Mullan M, Brown J, Crawford F, et al. (1991) Segregation of a missense mutation in the amyloid precursor protein gene with familial Alzheimer's disease. *Nature* 349: 704–706.
- Yoshioka K, Miki T, Katsuya T, Ogihara T, Sakaki Y (1991) The 717Val—Ile substitution in amyloid precursor protein is associated with familial Alzheimer's disease regardless of ethnic groups. *Biochem Biophys Res Commun* 178: 1141–1146.
- Mullan M, Crawford F, Axelman K, Houlden H, Lilius L, et al. (1992) A pathogenic mutation for probable Alzheimer's disease in the APP gene at the N-terminus of beta-amyloid. *Nat Genet* 1: 345–347.
- Sherrington R, Rogaev E, Liang Y, Rogaeva E, Levesque G, et al. (1995) Cloning of a gene bearing missense mutations in early-onset familial Alzheimer's disease. *Nature* 375: 754–760.
- Rogaev E, Sherrington R, Rogaeva E, Levesque G, Ikeda M, et al. (1995) Familial Alzheimer's disease in kindreds with missense mutations in a gene on chromosome 1 related to the Alzheimer's disease type 3 gene. *Nature* 376: 775–778.
- Levy-Lahad E, Wasco W, Poorkaj P, Romano D, Oshima J, et al. (1995) Candidate gene for the chromosome 1 familial Alzheimer's disease locus. *Science* 269: 973–977.
- Tamaoka A, Okada A, Ishibashi Y, Usami M, Sahara N, et al. (1994) APP717 missense mutation affects the ratio of amyloid beta protein species (A beta 1-42/43 and A beta 1-40) in familial Alzheimer's disease brain. *J Biol Chem* 269: 32721–32724.
- Citron M, Westaway D, Xia W, Carlson G, Diehl T, et al. (1997) Mutant presenilins of Alzheimer's disease increase production of 42-residue amyloid beta-protein in both transfected cells and transgenic mice. *Nat Med* 3: 67–72.
- Näslund J, Haroutunian V, Mohs R, Davis K, Davies P, et al. (2000) Correlation between elevated levels of amyloid beta-peptide in the brain and cognitive decline. *JAMA* 283: 1571–1577.
- Hsiao K, Chapman P, Nilsen S, Eckman C, Harigaya Y, et al. (1996) Correlative memory deficits, A beta elevation, and amyloid plaques in transgenic mice. *Science* 274: 99–102.
- Hsiao K (1998) Transgenic mice expressing Alzheimer amyloid precursor proteins. *Exp Gerontol* 33: 883–889.
- Hsiao K (2001) Learning and memory in transgenic mice modeling Alzheimer's disease. *Learn Mem* 8: 301–308.
- Chapman P, White G, Jones M, Cooper-Blacketer D, Marshall V, et al. (1999) Impaired synaptic plasticity and learning in aged amyloid precursor protein transgenic mice. *Nat Neurosci* 2: 271–276.
- Westerman M, Cooper-Blacketer D, Mariash A, Kotilinek L, Kawarabayashi T, et al. (2002) The relationship between Aβ and memory in the Tg2576 mouse model of Alzheimer's disease. *J Neurosci* 22: 1858–1867.
- Ushio C, Ariyasu H, Ariyasu T, Arai S, Ohta T, et al. (2009) Suppressive effects of a cyanine dye against herpes simplex virus (HSV)-1 infection. *Biomedical Research* 30: 365–368.
- Kunikata T, Ishihara T, Ushio S, Iwaki K, Ikeda M, et al. (2002) Lumin, a cyanine dye, enhances interleukin 12-dependent interferon gamma production by lipopolysaccharide-stimulated mouse splenocytes. *Biol Pharm Bull* 25: 1018–1021.
- Mito K (1996) Photodynamic efficiency of macrophage activity using a photosensitizer, lumin, with near-IR laser light for photoinmunotherapy of a cancer. *Frontiers of Medical and Biological Engineering* 7: 81–92.
- Sasaki Y, Nagai N, Okimura T (1987) Immunopharmacological actions of lumin (II): Effect of lumin administration in NZB × NZW (B/W) F1 mice. *Nippon Yakurigaku Zasshi* 89: 9–13.
- Sasaki Y, Nagai N, Okimura T, Yamamoto I (1987) Immunopharmacological actions of Lumin (I): Anti-allergic actions of Lumin. *Nippon Yakurigaku Zasshi* 89: 1–7.
- Ohta H, Arai S, Akita K, Ohta T, Fukuda S (2011) Neurotrophic Effects of a Cyanine Dye via the PI3K-Akt Pathway: Attenuation of Motor Discoordination and Neurodegeneration in an Ataxic Animal Model. *PLoS ONE* 6: e17137.
- Koya-Miyata S, Ohta H, Akita K, Arai S, Ohta T, et al. (2010) Cyanine photosensitizing dyes attenuate cerebral ischemia and reperfusion injury in rats. *Biol Pharm Bull* 33: 1872–1877.
- Ahmed S, Gogal RJ, Walsh JE (1994) A new rapid and simple non-radioactive assay to monitor and determine the proliferation of lymphocytes: an alternative to [<sup>3</sup>H] thymidine incorporation assay. *J Immunol Methods* 170: 211–224.
- Lashuel HA, Hartley DM, Balakhand D, Aggarwal A, Teichberg S, et al. (2002) New class of inhibitors of amyloid-β fibril formation. Implications for the mechanism of pathogenesis in Alzheimer's disease. *J Biol Chem* 277: 42881–42890.
- Rustay NR, Cronin EA, Curzon P, Markosyan S, Bitner RS, et al. (2010) Mice expressing the Swedish APP mutation on a 129 genetic background demonstrate consistent behavioral deficits and pathological markers of Alzheimer's disease. *Brain Res* 1311: 136–147.
- Maurice T, Lockhart BP, Privat A (1996) Amnesia induced in mice by centrally administered β-amyloid peptides involves cholinergic dysfunction. *Brain Res* 706: 181–193.
- Nagai T, Yamada K, Kim H, Kim Y, Noda Y, et al. (2003) Cognition impairment in the genetic model of aging klotho gene mutant mice: a role of oxidative stress. *FASEB J* 17: 50–52.
- Kurinami H, Sato N, Shinohara M, Takeuchi D, Takeda S, et al. (2008) Prevention of amyloid β-induced memory impairment by fluvastatin, associated with the decrease in amyloid β accumulation and oxidative stress in amyloid β injection mouse model. *Int J Mol Med* 21: 531–537.
- Shearman M, Ragan C, Iversen L (1994) Inhibition of PC12 cell redox activity is a specific, early indicator of the mechanism of β-amyloid-mediated cell death. *Proc Natl Acad Sci U S A* 91: 1470–1474.
- Ishihara M, Kadoma Y, Fujisawa S (2006) Kinetic radical-scavenging activity of platonin, a cyanine photosensitizing dye. *In Vivo* 20: 845–848.
- Suh YH, Checler F (2002) Amyloid precursorprotein, presenilins, and α-synuclein: Molecular pathogenesis and pharmacological applications in Alzheimer's disease. *Pharmacol Rev* 54: 469–525.
- Kogure K, Sassa H, Abe K, Kitahara K, Sano Y, et al. (1998) Inhibitory effects of pentamethine trinuclear cyanine dyes on ADP/Fe<sup>2+</sup>-induced lipid peroxidation in rat liver mitochondria: Changes in the mode of action with the hydrophobic nature of the dyes. *Biol Pharm Bull* 21: 180–183.
- Agdeppa E, Kepe V, Petri A, Satyamurthy N, Liu J, et al. (2003) In vitro detection of (S)-naproxen and ibuprofen binding to plaques in the Alzheimer's brain using the positron emission tomography molecular imaging probe 2-[1-6-[[2-[[[18F]fluoroethyl(methyl)amino]-2-naphthyl]ethylidene] malononitrile. *Neuroscience* 117: 723–730.
- Thomas T, Nadackal T, Thomas K (2001) Aspirin and non-steroidal anti-inflammatory drugs inhibit amyloid-beta aggregation. *Neuroreport* 12: 3263–3267.
- Levites Y, Smithson LA, Price RW, Dakin RS, Yuan B, et al. (2006) Insights into the mechanisms of action of anti-Aβ antibodies in Alzheimer's disease mouse models. *FASEB J* 20: 2576–2578.
- DeMattos R, Bales K, Cummins D, Dodart J, Paul S, et al. (2001) Peripheral anti-A beta antibody alters CNS and plasma A beta clearance and decreases brain A beta burden in a mouse model of Alzheimer's disease. *Proc Natl Acad Sci U S A* 98: 8850–8855.
- DeMattos R, Bales K, Cummins D, Paul S, Holtzman D (2002) Brain to plasma amyloid-beta efflux: a measure of brain amyloid burden in a mouse model of Alzheimer's disease. *Science* 295: 2264–2267.
- Rampon C, Tang Y, Goodhouse J, Shimizu E, Kynin M, et al. (2000) Enrichment induces structural changes and recovery from nonspatial memory deficits in CA1 NMDAR1-knockout mice. *Nat Neurosci* 3: 238–244.
- Winters B, Bussey TJ (2005) Glutamate receptors in perirhinal cortex mediate encoding, retrieval, and consolidation of object recognition memory. *J Neurosci* 25: 4243–4251.
- Phillips R, LeDoux JE (1992) Differential contribution of amygdala and hippocampus to cued and contextual fear conditioning. *Behav Neurosci* 106: 274–285.
- Wolfer DP, Müller U, Staglier M, Lipp HP (1997) Assessing the effects of the 129/Sv genetic background on swimming navigation learning in transgenic mutants: a study using mice with a modified β-amyloid precursor protein gene. *Brain Res* 771: 1–13.
- Gerlai R (1996) Gene-targeting studies of mammalian behavior: is it the mutation or the background genotype? *Trends Neurosci* 19: 177–181.
- Montkowski A, Poettig M, Mederer A, Hoslsboer (1997) Behavioral performance in three substrains of mouse strain 129. *Brain Res* 762: 12–18.
- VanDam D, Lenders G, DeDeyn PP (2006) Effect of Morris water maze diameter on visual-spatial learning in different mouse strains. *Neurobiol Learn Mem* 85: 164–172.
- Clapcote SJ, Roder JC (2004) Survey of embryonic stem cell line source strains in the water maze reveals superior reversal learning of 129S6/SvEvTac mice. *Behav Brain Res* 152: 35–48.
- Lesne S, Koh M, Kotilinek L, Kaye R, Glabe C, et al. (2006) A specific amyloid-beta protein assembly in the brain impairs memory. *Nature* 440: 352–357.
- Arendash G, Lewis J, Leightly R, McGowan E, Cracchiolo J, et al. (2004) Multi-metric behavioral comparison of APPsw and P301L models for Alzheimer's disease: linkage of poorer cognitive performance to tau pathology in forebrain. *Brain Res* 1012: 29–41.
- Horgan J, Miguel-Hidalgo JJ, Thrasher M, Bissette G (2007) Longitudinal brain corticotropin releasing factor and somatostatin in a transgenic mouse (TG2576) model of Alzheimer's disease. *J Alzheimers Dis* 12: 115–127.
- Morris R (1984) Developments of a water-maze procedure for studying spatial learning in the rat. *J Neurosci Methods* 11: 47–60.
- Save E, Poucet B (2000) Involvement of the hippocampus and associative parietal cortex in the use of proximal and distal landmarks for navigation. *Behav Brain Res* 109: 195–206.
- Nicoll MM, Prescott S, Bizon JL (2003) Emergence of a cuestrategy preference on the water maze task in aged C57B6 × SJL F1 hybrid mice. *Learn Mem* 10: 520–524.
- Clapcote SJ, Roder JC (2006) Deletion polymorphism of Disc1 is common to all 129 mouse substrains: Implications for gene-targeting studies of brain function. *Genetics* 173: 2407–2410. Sagare A, Deane R, Bell RD, Johnson B, Hamm K, et al. (2007) Clearance of amyloid-β by circulating lipoprotein receptors. *Nat Med* 13: 1029–1031.

52. Tomita K, Kubo K, Ishii K, Nakajima K (2011) Disrupted-in-Schizophrenia-1 (Disc1) is necessary for migration of the pyramidal neurons during mouse hippocampal development. *Hu Mol Genet* 20: 2834–2845.
53. Brightwell J, Smith C, Neve R, Colombo P (2007) Long-term memory for place learning is facilitated by expression of cAMP response element-binding protein in the dorsal hippocampus. *Learn Mem* 14: 195–199.
54. Zhu X, Raina A, Rotkamp C, Aliev G, Perry G, et al. (2001) Activation and redistribution of c-jun N-terminal kinase/stress activated protein kinase in degenerating neurons in Alzheimer's disease. *J Neurochem* 76: 435–441.
55. Cutler R, Kelly J, Storie K, Pedersen W, Tammara A, et al. (2004) Involvement of oxidative stress-induced abnormalities in ceramide and cholesterol metabolism in brain aging and Alzheimer's disease. *Proc Natl Acad Sci U S A* 101: 2070–2075.
56. Hensley K, Carmey J, Mattson M, Aksenova M, Harris M, et al. (1994) A model for  $\beta$ -amyloid aggregation and neurotoxicity based on free radical generation by the peptide: relevance to Alzheimer disease. *Proc Natl Acad Sci U S A* 91: 3270–3274.
57. Behl C, Davis J, Lesley R, Schubert D (1994) Hydrogen peroxide mediates amyloid beta protein toxicity. *Cell* 77: 817–827.
58. Mattson M, Goodman Y (1995) Different amyloidogenic peptides share a similar mechanism of neurotoxicity involving reactive oxygen species and calcium. *Brain Res* 676: 219–224.
59. Pillot T, Drouot B, Queille S, Labeur C, Vandekerckhove J, et al. (1999) The nonfibrillar amyloid  $\beta$ -peptide induces apoptotic neuronal cell death: involvement of its C-terminal fusogenic domain. *J Neurochem* 73: 1626–1634.
60. Gevais F, Xu D, Robertson G, Vaillancourt J, Zhu Y, et al. (1999) Involvement of caspases in proteolytic cleavage of Alzheimer's amyloid- $\beta$  precursor protein and amyloidogenic  $\text{A}\beta$ -peptide formation. *Cell* 97: 395–406.
61. Savory J, Rao J, Huang Y, Letada P, Herman MM (1999) Age-related hippocampal changes in Bcl-2: Bax ratio, oxidative stress, redox-active iron and apoptosis associated with aluminum-induced neurodegeneration: increased susceptibility with aging. *Neurotoxicology* 20: 805–817.